Performance analysis of 1300 nm SLEDs

Impact of temperature and length scaling

Author(s):
Loeser, Martin; Occhi, Lorenzo; Velez, Christian; Rezzonico, Raffaele; Witzigmann, Bernd

Publication date:
2006

Permanent link:
https://doi.org/10.3929/ethz-b-000035457

Originally published in:
Optical and Quantum Electronics 38(12-14), https://doi.org/10.1007/s11082-006-9012-1

Optical and Quantum Electronics (2006) 38:1069–1075
DOI 10.1007/s11082-006-9012-1

Performance analysis of 1300 nm SLEDs – impact of temperature and length scaling

MARTIN LOESER[1,*], LORENZO OCCHI[2], CHRISTIAN VÉLEZ[2], RAFFAELE REZZONICO[2] AND BERND WITZIGMANN[1]
[1]*Integrated Systems Laboratory, ETH Zurich, Gloriastrasse 35, CH-8032 Zurich, Switzerland;*
[2]*Exalos AG, Wagistr. 21, CH-8952 Schlieren, Switzerland.*
*(*author for correspondence: E-mail: loeser@iis.ee.ethz.ch)*

Received 30 August 2006; accepted 28 September 2006

Abstract. The impact of self-heating and cavity length on the spectral emission properties of SLEDs is investigated using a state-of-the-art simulation tool. Simulated data are compared to measurements for two InP-based benchmark devices operating around 1300 nm, and excellent agreement is achieved in either case.

Key words: Superluminescent LED, numerical simulation

1. Introduction

Super-luminescent light-emitting diodes (SLEDs) are an attractive light source in various fields of science and industry. Prominent applications are fiber-optic gyroscopes for satellite navigation or optical coherence tomography in cornea diagnostics. In most cases the market pull is towards broad ASE spectra (where *broad* refers to the 3 dB bandwidth) as well as high output power. As the physical processes that govern the device behavior are very complex comprehensive simulation tools allowing for electro-opto-thermal simulations are mandatory to minimize time-to-market and development costs.

2. Device physics

2.1. ELECTRO-THERMAL MODEL

The electro-thermal properties are described by a set of coupled partial differential equations (Selberherr 1984). The electrical problem is described elsewhere (Loeser *et al.* 2006); for thermal simulations the heat diffusion equation (1) is included. It reads

$$c_{\mathrm{tot}}\frac{\partial T}{\partial t} - \nabla(\kappa_{\mathrm{th}}\nabla T) = H, \tag{1}$$

where H denotes the heat sources considered in the model, i.e., Peltier heat, Joule heat, and (spontaneous) recombination heat – the impact of stimulated recombination on temperature is not considered. The inclusion of temperature effects adds an additional term $(\mu_n n P_n \nabla T)$ and $(\mu_p p P_p \nabla T)$ to the corresponding equations for the current densities $\mathbf{j}_n$ and $\mathbf{j}_p$. The recombination term, R, in the continuity equations can be decomposed as $R = R_{\text{spon}} + R_{\text{nr}} + R_{\text{st}}^{\text{ASE}}$, where the first term stands for radiative recombination, the second term denotes non-radiative recombination (Shockley-Read-Hall, Auger) and the last term is the stimulated recombination rate due to ASE and couples the optical problem to the electro-thermal model such that all solutions show full self-consistency.

2.2. ASE model

The ASE model accounts for the optical processes inside the device. Due to the tensorial geometry of the devices under investigation the 3D optical problem is decomposed into a 2D transverse and a 1D longitudinal problem. The full problem for the electric field E inside the cavity reads

$$\Delta E(\mathbf{x}, \omega) + \frac{\omega^2}{c^2} \epsilon_r E(\mathbf{x}, \omega) = F(\mathbf{x}, \omega), \tag{2}$$

where the spontaneous emission is modeled as a Langevin noise source. The electric field is then decomposed as

$$E(\mathbf{x}, \omega) = \sum_n \Psi_n(x, y) u_n(z, \omega). \tag{3}$$

The transverse eigenproblem for $\Psi_n(x, y)$ is solved using the Finite-Element Method (FEM) whereas the 1D problem for $u_n(z)$ is solved based on a Green's function approach (Henry 1986; Wenzel 2003). The stimulated recombination rate, $R_{\text{st}}^{\text{ASE}}$, can be obtained from E, and this closes the loop between the electro-thermal and the optical problem.

2.3. Gain and spontaneous emission

Optical gain and spontaneous emission are obtained with an additional software prior to the electro-opto-thermal simulation. In a first step the band structure is computed using a $8 \times 8\,\mathbf{k} \cdot \mathbf{p}$-method. The dephasing rates and the resulting optical gain are calculated utilizing the second Born approximation such that many-body effects as well as $\mathbf{k}$-dependent

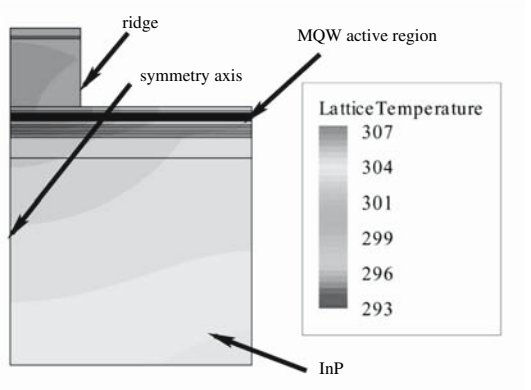

Fig. 1. Temperature distribution in the simulated 2D structure (in K). The drive current density is 8 kA/cm^2.

broadening are correctly being accounted for. The optical material gain is stored in a lookup table that is accessed by the device simulator.

3. Benchmark devices and simulated structures

The results obtained from the simulation software are compared to two existing devices manufactured by *EXALOS AG* (http://www.exalos.com). In both cases it is an InP-based edge-emitting SLED operating around 1300 nm. It features low facet reflectivities due to special anti-reflection coatings, and multi quantum-well (MQW) active regions sandwiched between two cladding layers. One device features a cavity length of 500 μm, the other of 950 μm. All simulations are carried out in 2D. The structure that is used for simulation is shown in Fig. 1.

4. Simulation results

After a careful calibration procedure the simulator reproduces all findings seen in electro-optical measurements. All calibration parameters, e.g., the Auger coefficient, are chosen to lie well within the range of what is reported in literature (Piprek 2003). As the benchmark devices are identical in every aspect but the length, the same set of material parameters is used for the two simulations.

For further analysis the focus lies on the spectra of the devices, as these quantities reveal more information than LI-curves (as the light power L is an integral quantity). Figures 2 and 3 show the simulated and computed

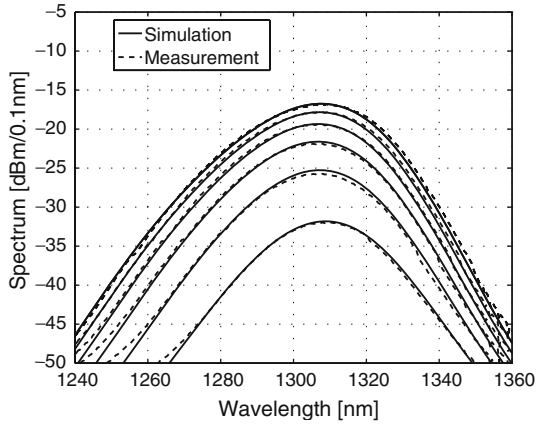

Fig. 2. ASE spectra for the 500 μm device. Dashed lines indicate measurements, solid lines stand for simulations. The spectra are compared for drive currents between 70 and 150 mA in steps of 20 mA. The 3 dB bandwidth is 32 nm in all cases.

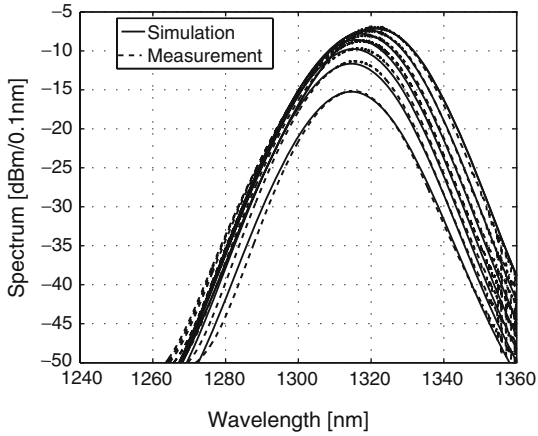

Fig. 3. ASE spectra for the 950 μm device. Dashed lines indicate measurements, solid lines stand for simulations. The spectra are compared for drive currents between 100 and 400 mA in steps of 50 mA. The 3 dB spectral width is 21 nm for each drive current.

output spectra of the two benchmark devices. The evolution of the output power level as well as the spectral shape are in excellent agreement with measurements. It has been shown in Loeser *et al.* (2006) that the spectral shape forms from a delicate combination of carrier distribution in the MQWs and the spectral gain shape of a single well. The inclusion of temperature effects further improves the agreement of simulated and measured data. Both devices show a constant 3 dB bandwidth for a large range of drive current densities. However, the position of the spectrum shifts with increasing drive current, as shown in Fig. 4.

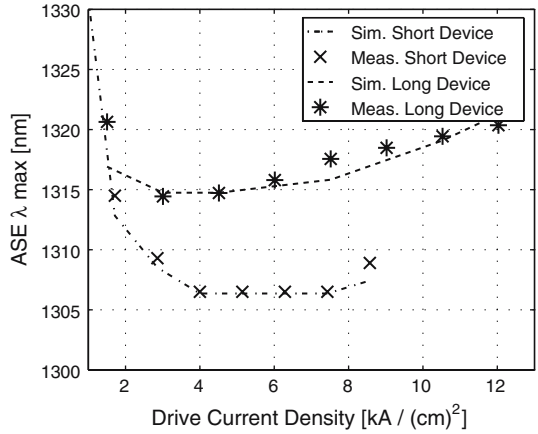

Fig. 4. Position of the ASE peak wavelength for various drive currents. The upper curve describes the behavior of the long device, the lower represents the short device.

Various physical mechanisms shift the emission spectra. An increase in the quantum well carrier densities leads to band-filling which, together with many-body effects, causes a blue shift of the spectrum. This effect is important because the carrier densities in the MQW active region are not pinned – as opposed to a laser – but change with the applied current. Bandgap narrowing due to Coulomb effects causes a red shift of the spectrum with increasing carrier population – this is included in the rigorous gain model described in Section 2.3. Self-heating due to Joule and recombination heat increases the device temperature and also leads to a red shift. Simulations reveal that this is the dominant mechanism for the devices under investigation as isothermal simulations lack any red shift. Both devices show very similar self-heating – the temperature difference in the active region of these two devices is only a few Kelvin. However, the red shift in the long device is more pronounced. This is because the short device shows a stronger increase in the MQW carrier densities with increasing current and the resulting blue shift compensates the temperature-induced red shift.

The following considerations focus on the impact of the cavity length on the emission characteristics. Figure 5 shows how bandwidth and output power evolve when the drive current density is kept constant at $7\,\mathrm{kA/cm^2}$ and the cavity length is increased from $500\,\mu\mathrm{m}$ to $1900\,\mu\mathrm{m}$. The decrease of the bandwidth with increasing cavity length can be attributed to the fact that both output power and stimulated recombination increase with cavity length. Therefore the quantum well carrier population in the long device is smaller at the same current density. This directly translates into narrower gain and spontaneous emission spectra. Second, the product of maximum gain and cavity length increases with increasing cavity length, and this also

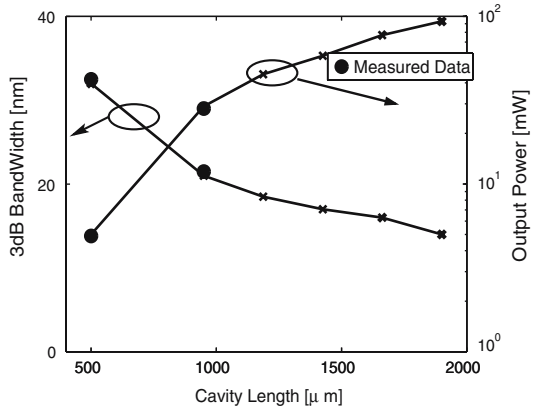

Fig. 5. Left: 3 dB bandwidth vs. cavity length. Right: total output power vs. cavity length. For the 500 μm and 950 μm cavity experimental data exists, marked with circles. The current density is kept constant at 7 kA/cm^2.

leads to narrower spectra. For SLEDs with low facet reflectivities the output power can be computed as

$$P = \int_{\omega} s(\omega) \exp(g(\omega)L) d\omega =: S \exp(GL), \tag{4}$$

where $s(\omega)$ stands for a source term due to spontaneous emission, $g(\omega)$ is the mode gain, and L denotes the cavity length. For the following S and G indicate an effective source and effective mode gain (Talli and Adams 2003). As $\log P \propto (GL)$, the slope of a semilogarithmic plot of output power versus cavity length is a measure for gain and accordingly for quantum well carrier population. The decreasing slope in Fig. 5 reveals that the long devices suffer from carrier depletion due to higher stimulated recombination. This underlines the great importance of the quantum well carrier population for overall device performance (Hybertsen *et al.* 2002).

5. Conclusion

Two-dimensional electro-opto-thermal simulations are carried out for transverse cuts of two edge-emitting SLEDs. Simulated emission properties are compared to measurements from two benchmark devices and excellent agreement is achieved in either case. The spectral properties of the devices are strongly affected by temperature and quantum well carrier population. The analysis of the cavity length as design parameter reveals the tradeoff between achievable output power and 3 dB bandwidth.

References

EXALOS Webpage, http://www.exalos.com.
Henry, Ch. *J. Lightwave Technol.* **4** 288, 1986
Hybertsen, M.S., B. Witzigmann, M.A. Alam and R.K. Smith. **1** 113, 2002
Loeser, M., L. Occhi, V. Laino and B. Witzigmann. Accurate modeling of gain and amplified spontaneous emission in super-luminescent LEDs, *Proc. SPIE*, 2006
Piprek, J. *Semiconductor Optoelectronic Devices*, Academic Press, San Diego, 2003
Selberherr, S. *Analysis and Simulation of Semiconductor Devices*, Springer, 1984
Talli, G. and M.J. Adams. *IEEE JQE* **39**, 2003
Wenzel, H. *IEEE J. Sel. Topics Quantum Electron*. **9**, 2003